

Quantum Computing for Power Flow Algorithms: Testing on real Quantum Computers

Brynjar Sævarsson, Spyros Chatzivasileiadis, Hjörtur Jóhannsson, Jacob Østergaard

Department of Wind and Energy Systems

Division of Electric Power and Energy

Technical University of Denmark

Kgs. Lyngby, Denmark

{brysa, spchatz, hjo, jaos}@dtu.dk

arXiv:2204.14028v1 [quant-ph] 29 Apr 2022

Abstract—

Quantum computing has the potential to solve many computational problems exponentially faster than classical computers. The high shares of renewables and the wide deployment of converter-interfaced resources require new tools that shall drastically accelerate power system computations, including optimization and security assessment, which can benefit from quantum computing. To the best of our knowledge, this is the first paper that goes beyond quantum computing simulations and performs an experimental application of Quantum Computing for power systems on a real quantum computer. We use four different quantum computers, apply the HHL quantum algorithm, and examine the impact of current noisy quantum hardware on the accuracy and speed of an AC power flow algorithm. Using the insights from our real experiments on a 3-bus system, we perform the same studies on a 5-bus system with a simulated quantum computer to identify challenges and open research questions related with the scalability of these algorithms.

Index Terms—power grids, power system security, quantum computing, quantum power flow

I. INTRODUCTION

The increasing penetration of distributed renewable energy sources (RES) brings a number of challenges when it comes to ensuring a secure operation of power systems. With traditional synchronous generation being replaced by thousands of converter-interfaced generation sources, the complexity of the power system greatly increases, its natural inertia decreases, and the dynamics of the system change. This means traditional offline methods for security assessment are expected to become insufficient as more detailed, and computationally demanding, simulations are required to capture the faster dynamics of RES. Additionally, the operating state of the system becomes subject to the prevailing weather conditions, making it difficult to predict hours ahead of time. The uncertainties introduced by RES can lead to exponentially more contingency scenarios needed to be considered to ensure N- x security. These challenges drive the need for new real-time and offline tools for security analysis. Assessing large complex systems for millions of contingency scenarios can be very computationally demanding and is currently one of the major challenges that utilities are expected to face in the future.

Over the last few years there has been a great leap in the area of Quantum Computing (QC), bringing us into the so called Noisy Intermediate-Scale Quantum (NISQ) era [1] of quantum

computing, where real quantum computers are already containing over 100 qubits. According to roadmaps of vendors such as IBM [2], there is ambitious development in building scalable quantum computers, with the aim of creating large-scale and noise-free devices in the near future. However, the current technology readiness level (TRL) of the NISQ-era quantum computers is still rather low and only very basic applications can be implemented. The use of quantum computations for power system applications is very new. Quantum power flow algorithms have been proposed to solve DC power flow [3] and AC power flow [4], and were tested with simulated quantum computers. The use of QC for contingency assessment was introduced in [5] and for performing EMT simulations in [6]. A common feature of these papers is the use of the HHL quantum algorithm for solving linear equations [7], as this promises exponential speedup compared to classical methods.

To the best of our knowledge, this paper presents the first implementation of an AC power flow on real Quantum Computers. The intention with the paper is to explore the current capabilities of QC for power flow studies and to investigate the foreseen future capabilities and practical implications of QC for power systems. We test our power flow algorithm for a simple 3 bus system on four of IBM's quantum computers to investigate the impact of noisy hardware. For larger systems, exceeding the current hardware capabilities of real quantum computers, we use a simulated quantum computer to investigate how the method scales with increasing system size. This is important for future implementations of full-scale power systems since the benefits of the computational power of quantum computing will be highly relevant for very large power systems.

This paper is organized as follows. Section II provides an overview of quantum computing and its potential for power systems. Section III describes the quantum power flow method and its implementation. In Section IV, we describe the simulation setup and the quantum hardware requirements. Section V provides the results of the power flow on both real and simulated quantum computers. In Section VI, we discuss potential issues with the scalability of the method. Section VII concludes.

II. THE POTENTIAL OF QUANTUM COMPUTING FOR POWER SYSTEMS

The way quantum computers function is fundamentally different from classical computers. Instead of using classical bits, which can only be in the states 0 and 1, quantum computers use quantum bits (qubits) which, in addition to being in states 0 and 1, can form a linear combination of states, i.e. have a certain probability to be measured either as 0 or 1. This state is referred to as superposition. While in superposition, they can also be said to be in all states simultaneously, i.e. both 0 and 1 or somewhere in-between, and only when measured do they collapse to 1 or 0 with some probability. An important feature of this is that the information contained in a quantum register grows exponentially for every qubit which is added [8]. That is, instead of requiring 2^n bits for a computing process with classical computing, quantum computing requires only n qubits. For example, if a process would require 1024 bits in a classical computer, a quantum computer would only need 10 qubits. Please bear in mind that currently publicly available quantum computers do not exceed 7 qubits. This means that we can perform computing processes that take up to 128 bits. Currently existing Quantum Computers (but not publicly available), on the other hand, go up to 100 qubits. This means they can handle processes up to $1.2 \cdot 10^{30}$ bits. That is a 30 orders of magnitude more powerful computer, while we have increased the number of qubits by only 1 order of magnitude.

Quantum states can also be used to evaluate functions for multiple values simultaneously. In a power systems context, such a feature can become extremely valuable for power flow analysis of multiple scenarios. Instead of sequentially solving a power flow to assess a large number generation and demand scenarios, future QC infrastructure could deliver the solution for many scenarios simultaneously, drastically accelerating e.g. the security assessment. This, and other special features of QC, allows them to solve certain problems exponentially faster than classical computers. Theoretically, Quantum Computers can solve all the same problems as classical computers; not all problems, though, allow for exponential speedups and in some cases QC are even slower than classical. QC is therefore seen as a supplement to classical computing for solving specific problems in a hybrid quantum-classical computation.

In the next sections, we present the formulation of the quantum power flow algorithm and the results we obtain after testing it on real quantum computers. Considering that the quantum computers that were accessible at the time of this paper only have 5 qubits, the application of our quantum power flow algorithm on real quantum computers is limited to a 3-bus system.

III. QUANTUM POWER FLOW METHOD

The implementation of the quantum power flow method we follow in this paper is based on the Fast Decoupled Load Flow (FDLF) method, which is a commonly used adaptation of the Newton Raphson Power Flow (NRPF). It exploits interdependence between $P - \theta$ and $Q - |V|$ to create two constant

Jacobian sub-matrices B' and B'' . This replaces one of the most computationally heavy parts of NRPF i.e. updating the Jacobian matrix in every iteration. FDLF converges to the same solution as NRPF since the mismatch functions are the same, but it usually requires more iterations than NRPF [9]. On the other hand, each iteration of FDLF is much faster, meaning that the overall computation time of FDLF can often be quite faster, especially for large system. In each iteration, we solve equations (1)-(3) for $\Delta\theta$ and ΔV_m until the norm of ΔP and ΔQ is less than the chosen tolerance ξ .

$$\Delta S = (S_{bus} - \mathbf{V} \circ \overline{(Y_{bus} \cdot \mathbf{V})}) \oslash V_m \quad (1)$$

$$\Delta P = \Re(\Delta S_{pv+pq}) = B' \Delta\theta \quad (2)$$

$$\Delta Q = \Im(\Delta S_{pq}) = B'' \Delta V_m \quad (3)$$

In (1)-(3), $\mathbf{V} = V_m \angle \theta$ is a vector collecting the voltage phasors for all buses, \circ and \oslash denote the element-wise product and division respectively, and pv and pq are indices corresponding to the set of PV and PQ buses respectively. The structure of FDLF makes it very suitable for hybrid classical-quantum computing since we can easily replace the numerical algorithm solving equations (2) and (3) with a method which is capable of running on a quantum computer. HHL is probably the most popular quantum algorithm for solving a set of linear equations at the moment, with a runtime of $\mathcal{O}(\log(N) \frac{s^2 \kappa^2}{\epsilon})$ [7]; here, N is the number of equations, s is the sparsity and κ the condition number of the system matrix, and ϵ is the solution accuracy. In theory, HHL can achieve an exponential speedup over the fastest classical algorithm, which is the conjugate gradient method and has a runtime of $\mathcal{O}(N s \kappa \log(\frac{1}{\epsilon}))$.

A system of linear equations is usually given in the form:

$$Ax = b, \quad (4)$$

where given a known matrix A and vector b , we solve for x . For quantum systems we use the Dirac (or bra-ket) notation, where we denote a vector with a **ket** which has the form $|v\rangle$ and represents the state of a quantum system. We also denote a **bra** with the form $\langle v|$, where bra is the conjugate transpose of ket. Quantum vectors are often very sparse i.e. with most amplitudes equal to zero and this notation makes it much simpler to represent values of interest.

We rescale the system in (4) by normalizing x and b , and we can then map them to the quantum states $|x\rangle$ and $|b\rangle$.

$$A|x\rangle = |b\rangle \quad (5)$$

Portraying equation (2) in this form we get:

$$B' |\Delta\theta\rangle = |\Delta P\rangle \quad (6)$$

If we express the right hand side in the eigenbasis of the B' matrix, we can write it as:

$$|\Delta P\rangle = \sum_{j=0}^{N-1} \Delta P_j |u'_j\rangle \quad (7)$$

The HHL method requires the matrix A to be Hermitian, that is equal to its conjugate transpose, which happens to be the case for B' and B'' of FDLF. And since the matrices are Hermitian, they have a spectral decomposition:

$$B' = \sum_{j=0}^{N-1} \lambda'_j |u'_j\rangle \langle u'_j| \quad (8)$$

$$B'^{-1} = \sum_{j=0}^{N-1} \lambda'^{-1}_j |u'_j\rangle \langle u'_j| \quad (9)$$

Where λ'_j and u'_j are the j_{th} eigenvalue and eigenvector of the B' matrix. Putting (6), (7) and (9) together we then get:

$$|\Delta\theta\rangle = B'^{-1} |\Delta P\rangle = \sum_{j=0}^{N-1} \lambda'^{-1}_j \Delta P_j |u'_j\rangle \langle u'_j| |u'_j\rangle \quad (10)$$

As the scalar product $\langle u'_j | u'_j \rangle = 1$, (10) simplifies to:

$$|\Delta\theta\rangle = \sum_{j=0}^{N-1} \lambda'^{-1}_j \Delta P_j |u'_j\rangle \quad (11)$$

And following the same procedure for ΔV_m and B'' we get:

$$|\Delta V_m\rangle = B''^{-1} |\Delta Q\rangle = \sum_{j=0}^{N-1} \lambda''^{-1}_j \Delta Q_j |u''_j\rangle \quad (12)$$

To solve (11) a quantum circuit is implemented as shown in Fig. 1. This circuit is for solving a 2x2 system of equations, i.e., $N = 2$. It consists of three registers, nb , nl , na , which are all initialized as $|0\rangle$. nb is the data register where we load the data vector b (here $b \equiv \Delta P$ onto $\log_2(N) = 1$ qubits:

$$|0\rangle \mapsto |\Delta P\rangle \quad (13)$$

Next, we apply quantum phase estimation to estimate the eigenvalues of the B matrix. The nl register consists of 3 qubits where we store the approximation of the eigenvalues $|\tilde{\lambda}_j\rangle$. The more qubits used in nl , the more accurately we can estimate the eigenvalues of B . The last register, na , consists of a single auxiliary qubit. The output auxiliary qubit indicates if we can obtain a binary estimation of the eigenvalues and the data vector, i.e. if we can trust their numerical result when we measure them, or not. To get the output of the auxiliary qubit, we perform a rotation conditioned on $|\tilde{\lambda}_j\rangle$, and finally an inverse phase estimation. When we measure the output of the auxiliary qubit as 1, then the registers nb , nl are in the post measurement state; this means that the phase estimation outputs a binary estimation of the eigenvalues of the B matrix, and after an inverse phase estimation, the nb register contains the solution $|\Delta\theta\rangle$. For more information about the steps of the HHL algorithm, the interested reader can refer to [7].

The implemented Quantum Power Flow (QPF) algorithm is shown in Algorithm 1.

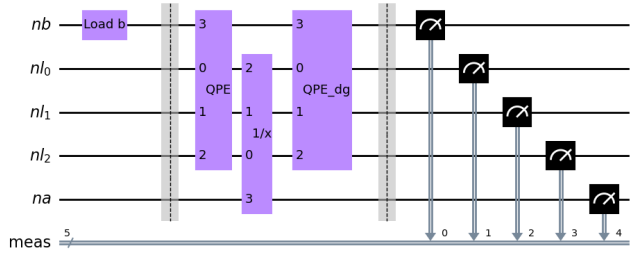


Fig. 1: Quantum HHL circuit used for solving a Quantum Power Flow (QPF) on a 3-bus system. The blocks shown in the circuit are: Preparation of the data vector (Load b), Quantum Phase Estimation (QPE), conditioned rotation ($1/x$) and inverse QPE (QPE_{dg}). Finally, each qubit is measured and the result is stored in a classical 5 bit register where meas 0 is the least significant bit and meas 4 is the most significant bit.

Algorithm 1 Quantum Power Flow

```

Input  $Y_{bus}, B', B'', V_0, S_{bus}$ 
Update  $\Delta P, \Delta Q$ 
while  $\|\Delta P\| \geq \xi$  AND  $\|\Delta Q\| \geq \xi$  do
     $\Delta\theta = HHL(B', \Delta P)$ 
     $\Delta V_m = HHL(B'', \Delta Q)$ 
    Update  $V_m \angle \theta$ 
    Update  $\Delta P, \Delta Q$ 
end while
return  $V_m \angle \theta$ 

```

IV. SIMULATIONS

The capabilities of both real and simulated Quantum Computers are still limited. Some simplifications must therefore be made to run the power flow algorithm on a real quantum computer. If the eigenvalues of the system matrix cannot be exactly represented by nl bits, the quantum phase estimation will only give an approximation of the eigenvalues λ_j of the B' and B'' matrices; this introduces an error in the results. In order to investigate the performance of real quantum computers, at this stage, we select the parameters of the test systems so that each of the eigenvalues of the B matrices can be closely represented by a $nl = 3$ bits. As our focus is to test a simple system on a real QC, for the purpose of the investigations in this paper we also consider only slack and PQ buses, and no phase-shifting transformers. This means that $B' = B''$, and we can use the same HHL circuit for both (??) and (12) only with a different vector b loaded onto the nb register (i.e., $\Delta\theta$ or ΔV). The two power systems considered for this paper are shown in Fig. 2 and the parameters of the 3-bus system are shown in Table I.

The parameters in Table I give the B matrices:

$$B' = B'' = \begin{bmatrix} -1.5 & 0.5 \\ 0.5 & -1.5 \end{bmatrix} \quad (14)$$

The eigenvalues of matrices B' and B'' are $\{-1, -2\}$.

systems/3bus system
 (a) Three bus system
 systems/5bus system
 (b) Five bus system
 Fig. 2: Systems for testing Quantum Power Flow (QPF).

TABLE I: Three bus system parameters

Bus	Type	P _{MW}	Q _{MVAr}	V _{pu}	θ°
1	Slack	5	6.9	1.03	0
2	PQ	10	0	1.012	2.109
3	PQ	-15	-5	0.985	-4.996
Line	From	To	R _{pu}	X _{pu}	
1	1	2	0	1j	
2	1	3	0	1j	
3	2	3	0	2j	

A. Quantum hardware requirements

The number of qubits (circuit width) required for the HHL circuit depends on the required accuracy of the phase estimation and the number of variables in the data vector (plus the auxiliary qubit that we always need to indicate if we have obtained a binary estimation or not). For example, the 3-bus system has 2 variables for ΔP which are encoded in 1 qubit ($\#qubits = \log_2 N$, where N is the number of variables, as mentioned in Section II) and we use a 2-bit estimation of the eigenvalues of B' . Another qubit is needed for the phase estimation in case the system matrix has negative eigenvalues. Including the auxiliary qubit, this gives a total of 5 qubits required for the 3-bus system. The qubit for negative eigenvalues could be eliminated if we can assume all eigenvalues have the same sign. This is, however, not always the case for larger power systems which could for example include capacitive branches.

We shall note here that the true benefits of Quantum Computing emerge in large systems, since the number of required qubits have a sublinear increase with larger system sizes (logarithmic to be precise). This means that we can represent very large systems with only a few qubits. For example, applying the $\log_2(N)$ rule for the required number of qubits, we can represent the data vector of a 500'000-bus system with only 20 qubits ($2^{20} = 1'048'576 \approx 2 \times 500'000$ values).

Currently, however, the major issue with scalability is not as much the circuit width, i.e. the number of qubits, but the circuit depth; that is, the number of gates in the quantum circuit, as shown in Fig. 1. The current general implementation of the HHL algorithm uses methods which scale exponentially with the number of qubits, and, so far, no algorithm exists for preparing the HHL circuit with polynomial resources for an arbitrary matrix. Table II shows how the circuit sizes grow with the matrix size.

V. SIMULATION RESULTS

A. 3-bus system on real Quantum Computers

The power flow application is implemented with IBM's qiskit (0.34.1). The 3-bus system is tested on 4 of IBM's open

TABLE II: Quantum Circuit Sizes

	3 bus	5 bus	9 bus	17 bus
B' matrix size	2x2	4x4	8x8	16x16
Circuit Width	5	7	9	11
Circuit Depth	336	3528	76876	802737
CNOT Gates	108	1181	28956	298594

access quantum computers [10] listed in Table III: ibmq_lima, ibmq_belem, ibmq_quito, and ibmq_bogota.

TABLE III: Quantum Computers used for testing Quantum Power Flow (values taken on 23.02.2022)

QC	Qubits	QV	avg. CNOT error
ibmq_lima	5	8	9.996e-3
ibmq_belem	5	16	1.363e-2
ibmq_quito	5	16	1.135e-2
ibmq_bogota	5	32	1.206e-2

The results of the 3-bus power flow for each iteration of the power flow calculation on ibmq_quito are shown in Table IV. The rest of the quantum computers we used, i.e. ibmq_lima, ibmq_belem, and ibmq_bogota give similar results. The Quantum Power Flow converges to the same solution as the classical FDLF but, due to the noisy hardware available at the moment, it requires a much larger number of iterations. With the tolerance set to 10^{-5} , the classical method converges in 5 iterations while the Quantum Power Flow (QPF) takes around 32-38 iterations.

Since the available quantum software (qiskit 0.34.1) does not allow us to implement if-loops, for-loops, and while-loops within a real quantum algorithm at the moment (March 2022). As a result, implementing a numerical solution algorithm requires us to extract the value of the quantum data vector in every iteration, perform the logical operations (e.g. is $\Delta P \geq \xi$, see Algorithm 1) and plug ΔP back in the quantum circuit again for the next iteration. Considering that the data vector is in a quantum state, we need to "probe" ΔP multiple times to measure the probability distribution of the solution. This requires time of at least $\mathcal{O}(N)$ (see also the Discussion in Section VI). Obviously, this slows down considerably our quantum algorithm at the moment. The next qiskit version, which is expected around August 2022, is expected to allow for extended functionality; this will unleash a wide range of opportunities, including if-clauses, for-loops, and while-loops inside the quantum algorithm which could eliminate the need for measuring the data vector in each iteration of the QPF.

Going back to the currently possible implementation of our QPF, where the data vector ΔP needs to be measured in every iteration, Fig. 3 shows the measurement from the first iteration with and without noise. The values of ΔP are read from the states where the auxiliary qubit is 1, i.e. "10000" and "10001" in the histogram.

An estimate of $\Delta\theta$ is extracted from the measured probabilities in Fig. 3.

$$\Delta\theta \approx \|\Delta P\| * \sqrt{\text{probability}} \quad (15)$$

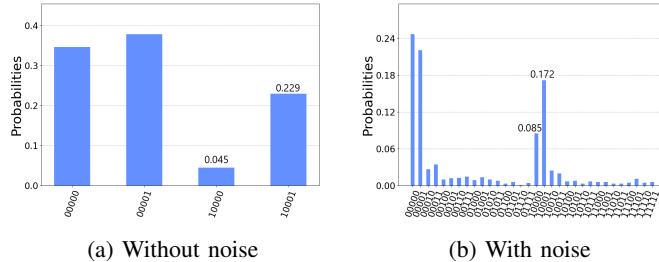


Fig. 3: Histogram showing measurements of $|\Delta\theta|$ in the first iteration. The values of $\Delta\theta$ are estimated from the probability distribution read from the data register nb in Fig. 1 when the auxiliary bit $na = 1$ i.e. from the states "10000" and "10001"

TABLE IV: Iterations of Classical FDLF vs QPF on ibmq_quito

FDLF iteration	V_2	θ_2	V_3	θ_3
1	1.01750000	2.14859173	0.99250000	-5.01338071
2	1.01198104	2.08682333	0.98513520	-4.94593291
3	1.01210909	2.10823443	0.98510531	-4.99645096
4	1.01200181	2.10832465	0.98496362	-4.99531212
5	1.01200181	2.10872362	0.98496362	-4.99629051
QPF iteration	V_2	θ_2	V_3	θ_3
1	1.00602829	2.05419579	0.99405120	-1.77164967
2	1.00937372	3.12147980	0.99099606	-2.73581045
3	1.01129425	2.50579482	0.04373437	-3.30344432
⋮	⋮	⋮	⋮	⋮
34	1.01200263	2.10882674	0.98496970	-4.99558292
35	1.01200492	2.10901696	0.98496697	-4.99577486

For the first iteration of the noise free simulation, this gives:

$$\begin{bmatrix} \Delta\theta_2 \\ \Delta\theta_3 \end{bmatrix} \approx 0.1803 * \begin{bmatrix} \sqrt{0.045} \\ \sqrt{0.229} \end{bmatrix} \approx \begin{bmatrix} 0.03824 \\ 0.08628 \end{bmatrix} \quad (16)$$

Where $\|\Delta P\| = 0.1803$. We can see that the result of the noise-free quantum simulation is very close to the result for the first iteration of the classical computing algorithm, which is $\Delta\theta = [0.0375, 0.0875]$ rad. On the contrary, for noisy quantum computations, which are based on real quantum computers, the output is $\Delta\theta = [0.0526, 0.0748]$ rad after the first iteration. This is the reason why noise-free quantum computing converges almost equally fast as classical computing (same number of iterations, see Fig. 4), while the algorithms implemented on actual quantum computers require at the moment a significantly larger number of iterations.

A comparison between the convergence of the classical method, the 4 physical QC devices and a simulated noise-free QC is shown in Fig. 4. It shows how a simulated noise-free QC gives close to identical results with a classical computer, while the real noisy QCs converge much slower. As the reader observes, there is not a notable difference between the implementations on the 4 real QCs.

B. 5-bus system

We test our QPF on a 5-bus system. Our goal is to investigate how current noisy hardware impact the Quantum

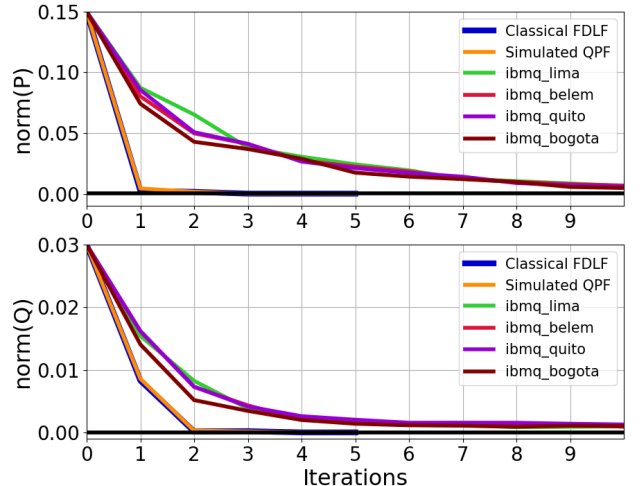


Fig. 4: Power flow convergence of the 3-bus system

Power Flow solution as we scale to larger systems. As shown in Table II, a QPF for a 5-bus system requires 7 qubits and a much larger number of gates. This makes it unfortunately unfeasible to test it in current QC hardware that researchers are able to access. To be as close to a real implementation as possible, we use a simulated quantum computer and include the actual noise characteristics of ibmq_lima in our implementation. As all real Quantum Computers we tested demonstrate a similar performance (see Fig. 4), we would obtain a similar performance if we had used the noise characteristics of any other QC (i.e. ibmq_belem, ibmq_quito, ibmq_bogota).

Similar to the 3-bus system, the line parameters of the 5 bus system are chosen so the eigenvalues of the \mathbf{B} matrices can be closely represented by 3 bits, as our primary focus is to examine the impact of the noisy quantum hardware. The \mathbf{B} matrices are presented in (17). Fully acknowledging though that the characteristics of real power systems can vary significantly, in our experiments we also perturb the system characteristics (and the \mathbf{B} matrices shown in (17)) to explore cases where \mathbf{B} matrices result to eigenvalues that cannot be accurately represented by 3 bits (see Fig. 5).

$$\mathbf{B}' = \mathbf{B}'' = \begin{bmatrix} -4 & 0.03 & 0 & 0 \\ 0.03 & -3 & 0.02 & 0 \\ 0 & 0.02 & -1.55 & 0.5 \\ 0 & 0 & 0.5 & -1.45 \end{bmatrix} \quad (17)$$

The eigenvalues of \mathbf{B}' and \mathbf{B}'' in this case are $\{-1, -2, -3, -4\}$.

Figure 5 shows the iterations of the 5-bus power flow. As with the 3-bus system, it converges to the correct solution and the noise-free simulation is very close to the classical one. When we alter the line parameters, so that the eigenvalues of the \mathbf{B} matrices cannot be represented exactly by 3 bits, we observe that this introduces a small delay in the convergence (red line in Fig. 5), but it is still relatively small. The major difference in convergence speed emerges when we add the noise characteristics in the computation (green line in Fig. 5).

As before, the presence of noise greatly impacts the number of iterations required. The larger number of gates required for the circuit compared to the 3-bus system also means greater impact from the noise, as each gate adds noise to the result. Our simulations show that unless we develop low-noise quantum hardware, it would be challenging to perform computations for larger systems.

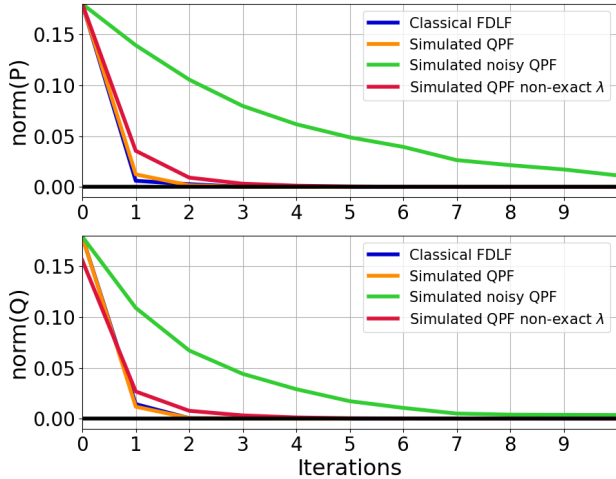


Fig. 5: Power flow convergence of the 5-bus system

Based on the findings from our experiments, in the next section, we discuss opportunities and challenges arising from the development of quantum algorithms for power system applications.

VI. DISCUSSION

The result given by the HHL algorithm is encoded as a quantum state. If we want to extract the full state vector from the quantum state we need time of at least $\mathcal{O}(N)$. Therefore, if we do this in every iteration of our power flow we lose any benefit of the quantum speedup [11]. For an HHL-based AC QPF to achieve quantum advantage, the whole iteration process would likely have to be performed by the QC and we would only extract the final result. To do that, we need a quantum memory to store the quantum state between iterations so we can update our power mismatches; this is not yet available in current real QC machines, but it is expected to exist in the future. The next version of qiskit is expected to include some form of looping capabilities which will greatly improve what we are capable of doing with our quantum algorithms.

Assuming we have quantum memory, extracting the final result can still reduce the speedup of QC. However, it is also possible to obtain some limited statistical information, such as the presence of very high values, from the HHL algorithm without extracting the full solution vector. This could be useful for contingency assessment where we have a large number of scenarios and only want to identify the ones that are unstable or overloaded.

For the HHL algorithm to be efficient, the B matrix should be well-conditioned. As B is Hermitian, the condition number

is given by the ratio between the largest and smallest eigenvalue $\kappa = \frac{|\lambda_{\max}|}{|\lambda_{\min}|}$. If κ grows significantly with the size of B, then the exponential speedup of HHL is lost [11]. As shown in Fig. 6, the condition number seems to grow exponentially for larger test cases. This means that we need to perform a preprocessing procedure to the system matrices to reduce their condition number while maintaining their characteristics, before plugging them in a Quantum Computer, if we wish to maintain the quantum advantage. Further research is required on how to achieve that in order to enable efficient quantum computations.

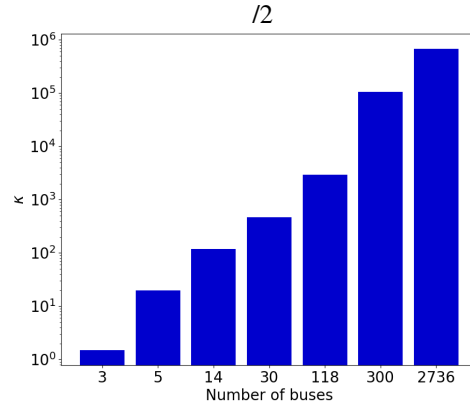


Fig. 6: Condition number κ of B' for 6 IEEE test systems (3 - 300 buses) and the 2736-bus Polish system.

The quantum power flow converges to the correct solution even with current noisy hardware. However, the high number of iterations required could make it challenging to achieve quantum advantage while quantum computers have a high level of noise.

This implementation of QPF aims to adapt the classical FDLF method to run on a quantum computer. As shown in this paper, there is a number of challenges with current available hardware and the lack of quantum memory. However, since quantum computers are fundamentally different from classical computers, future implementations of QPF might even take a different approach in order to better utilize the unique capabilities of QC of evaluating multiple values simultaneously and possibly avoid the iterative process altogether. This would require further research.

VII. CONCLUSION

In this paper, we have successfully implemented and tested a quantum power flow application on real Noisy-Intermediate-Scale-Quantum-era (NISQ-era) quantum computers. We have shown that current hardware is capable of performing a power flow for small test systems, but scalability is currently a major issue. There are still many challenges which must be resolved before practical quantum power flow applications can achieve quantum advantage. However, with further development and increasing capabilities of quantum computers, quantum applications for power systems could become extremely useful for future power system analysis.

REFERENCES

- [1] J. Preskill, "Quantum computing in the nisq era and beyond," *Quantum*, vol. 2, p. 79, Aug 2018. [Online]. Available: <http://dx.doi.org/10.22331/q-2018-08-06-79>
- [2] "Ibm's roadmap for scaling quantum technology," <https://research.ibm.com/blog/ibm-quantum-roadmap>, 2020.
- [3] R. Eskandarpour, K. Ghosh, A. Khodaei, and A. Paaso, "Experimental quantum computing to solve network dc power flow problem," 2021.
- [4] F. Feng, Y. Zhou, and P. Zhang, "Quantum power flow," 2021.
- [5] R. Eskandarpour, P. Gokhale, A. Khodaei, F. T. Chong, A. Passo, and S. Bahramirad, "Quantum computing for enhancing grid security," *IEEE Transactions on Power Systems*, vol. 35, no. 5, pp. 4135–4137, 2020.
- [6] Y. Zhou, F. Feng, and P. Zhang, "Quantum electromagnetic transients program," *IEEE Transactions on Power Systems*, vol. 36, no. 4, pp. 3813–3816, 2021.
- [7] A. W. Harrow, A. Hassidim, and S. Lloyd, "Quantum algorithm for linear systems of equations," *Phys. Rev. Lett.*, vol. 103, p. 150502, Oct 2009. [Online]. Available: <https://link.aps.org/doi/10.1103/PhysRevLett.103.150502>
- [8] M. A. Nielsen and I. L. Chuang, *Quantum Computation and Quantum Information: 10th Anniversary Edition*, 10th ed. USA: Cambridge University Press, 2011.
- [9] B. Stott and O. Alsac, "Fast decoupled load flow," *IEEE Transactions on Power Apparatus and Systems*, vol. PAS-93, no. 3, pp. 859–869, 1974.
- [10] "Ibm quantum." <https://quantum-computing.ibm.com/>, 2022.
- [11] S. Aaronson, "Read the fine print," *Nature Physics*, vol. 11, no. 4, pp. 291–293, Apr 2015. [Online]. Available: <https://doi.org/10.1038/nphys3272>